CrossMark

ORIGINAL PAPER

Experimental Investigation on the Bearing Capacity of Stone Columns with Granular Blankets

N. Mehrannia · J. Nazariafshar · F. Kalantary

Abstract Using stone columns is an efficient method to increase the bearing capacity of soft soils. This has led to an increased interest in further developing and improving the method. In addition, granular blankets are used to increase the bearing capacity of the stone columns. In this research, the bearing capacity of stone columns, granular blankets, and a combination of both methods in reinforced and unreinforced modes was examined using large-scale laboratory tests. A scale factor of 1–10 is used for the geometry of the models, and the stone columns are a floating type that are 60 mm in diameter and 350 mm in length. These columns are either reinforced with vertical encasement of a geotextile or they are unreinforced. The granular blankets are either reinforced by using a biaxial geogrid or they are unreinforced with 40 and 75 mm thicknesses. In general, 16 large experimental tests have been carried out. Results indicate that using all these variations (granular blankets, stone columns, and a combination of both) improves bearing capacity. Using geogrid as the reinforcement of granular blankets and geotextile as stone-column encasement increases the efficiency of granular blankets and stone columns significantly. The maximum bearing capacity was obtained when reinforced granular blankets and reinforced stone columns were combined. The stress-concentration ratio and bearing capacity increased as geotextile encasement was used in the stone columns.

Keywords Stone columns · Granular blanket · Bearing capacity · Reinforcement · Ground improvement

1 Introduction

Using stone columns is a useful, cost-effective, and environmentally friendly method for resolving low bearing capacity and large-scale settlement of soft soil. Stone columns are created by replacing poor soil with sand or a combination of sand and crushed stones to construct a vertically resistant system. The application of the reinforced soil blankets has long been discussed. The role of geosynthetic reinforcement of soil in improving the bearing capacity has been investigated by several researchers, such as Akinmusuru and Akinbolade (1981), Guido et al. (1985), Yetimoglu et al. (1994); Fakher and Jones (1996); Patra et al. (2005), Zidan (2012). Most of the bearing capacity of stone columns is caused by the lateral confining

N. Mehrannia
Department of Civil Engineering, Science and Research Branch, Islamic Azad University, Tehran, Iran

J. Nazariafshar
Department of Civil Engineering, Shahr-e-Qods Branch, Islamic Azad University, Tehran, Iran

F. Kalantary (✉)
K. N. Toosi University of Technology, Tehran, Iran
e-mail: fz_kalantary@kntu.ac.ir

pressure of the surrounding soil, and it remains stable because of the pressure imposed by the soil around the stone columns (Greenwood 1970; Barksdale and Bachus 1983; Gniel and Bouazza 2008; Nazariafshar and Ghazavi 2014). Sufficient lateral confinement may not be available in the case of very soft clays having low undrained shear strengths (cu < 15 kPa) (Raithel et al. 2002; Murugesan and Rajagopal 2006, 2010; Mohapatra et al. 2016). Thereby, another element is needed to increase lateral confining pressure. Van Impe (1989) proposed geosynthetic encasement to increase the bearing capacity of the stone columns for the first time. In fact, the lateral confining pressure increased using geotextile around the stone columns. Geotextile prevents granular materials of stone columns from sinking into the soft soil, and—as a result— bearing capacity increases significantly. The concept of encasing granular columns with geosynthetics to increase their capacity has been acknowledged by numerous researchers (Murugesan and Rajagopal 2006; Yoo 2010; Deb et al. 2010; Yoo and Lee 2012; Zhang et al. 2012; Almeida et al. 2013; Dash and Bora 2013b; Elsawy 2013; Ghazavi and Nazariafshar 2013; McCabe et al. 2013; Ali et al. 2014; Hong et al. 2016; Miranda and Costa 2016). The length-to-diameter ratio of the stone columns is an important factor in the design of the stone columns. The bearing capacity increases as the length-to-diameter ratio of the stone columns increases. However, when a certain length-to-diameter ratio is achieved, no significant increase is observed in bearing capacity. In several studies, the optimal length-to-diameter ratio in the stone columns varied from 5 to 8. (Hughes and Withers 1974; Rao et al. 1992; Mckelvey et al. 2004; Sivakumar et al. 2011). Muir Wood et al. (2000) showed that the optimal length-to-diameter ratio depends on the stone column area ratio and on such parameters as the stiffness, strength, and density of the stone column materials and the soil around the stone columns. Many studies have been investigated on various types of failure in stone columns. Generally, there are three types of these failures: (1) lateral expansion (bulging), (2) general shear, and (3) punching shear. Most failures in stone columns occur because of lateral expansion. Many studies have been conducted on this type of failure (Greenwood 1970; Vesic 1972; Hughes and Withers 1974; Datye and Nagaraju 1975; Madhav et al. 1979). General shear occurs in short stone columns that rely on a hard bed. Wong (1975), Madhav and Vitkar (1978), and Barksdale and Bachus (1983)

studied this type of failure. Punching shear occurs in the construction of short stone columns and relies on soft soil. Aboshi et al. (1979) studied this type of failure. Babu et al. (2013) discusses the techniques and methods of construction of stone columns, mechanisms of stone column behavior under load and associated design philosophies along with some practical findings from recent research programs. Stuedlein and Holtz (2013) developed a multiple linear regression model for the prediction of footing displacements for aggregate pier reinforced clay under a wide range of pier configurations and soil conditions. This method was shown to predict bearing pressures over a range of typical design displacements (i.e., up to 50 mm), pier configurations, and shear strengths.

Andreou and Papadopoulos (2014) studied factors affecting the settlement estimation of stone column reinforced soils. They proposed analytical method, governed by the failure mechanism of a cylindrical cone and concluded that the beneficial effect of this ground improvement technique, especially on the foundation soil with the lower strength characteristics, is more pronounced. Problems of similarity between reduced-scale models and equivalent field-scale prototypes led to uncertainty about whether the behavior and mechanisms observed in reduced-scale models are typical of the field-scale prototype. Iai (1989), Baker et al. (1991), Dash and Bora (2013a) and Hong et al. (2016) report similarities between reduced-scale models and equivalent field-scale prototypes.

The length of the stone columns is not deep enough to get to the stiff layer, and in most cases the stone column is a floating type. In most previous studies, the stone columns were placed on a rigid bed, and the effect of the floating stone columns was less examined. Also, in most projects the performance of encased stone columns is difficult, so we considered using a stone column with a blanket layer instead of the encased stone columns. Thus, in this study, the use of large-scale laboratory tests examined the bearing capacity of floating stone columns with reinforced or unreinforced granular blankets.

1.1 Experimental Setup and Test Procedure

A large test chamber with dimensions of 1.2 m × 1.2 m in plan and 0.9 m in height was used for the experimental studies. The dimensions of the

stone columns were 60 mm in diameter and 350 mm in length, and a length-to-diameter ratio of 5.8 was considered constant in all tests. Mayerhof and Sastry (1978) observed that the failure zone below a rigid pile extends over a depth of approximately 2 times its diameter. Because the stone columns are flexible, this depth would be less. Selig and McKee (1961) and Chummar (1972) indicated that the failure wedge in the foundation bed extends over a distance of approximately 2–2.5 times the footing width (D), away from its center. In the present study, the diameter of the loading plate is 20 cm, and the distance of the chamber walls from the center of the footing is approximately 3D, so the failure wedge does not interfere with the chamber walls. To prevent deformation in the boundary of the experimental box, the walls were made stiff on all sides. Soft clay construction was done by a unit weight-control method, and the box walls were graded in 5 cm intervals. The soft clay layers were filled into the box in layers with a 5 cm thickness, and then compacted. The loading systems consist of the loading frame, the server motor, the loading plate, and the data-acquisition system. The loading was applied based on the displacement-control method at a rate of 1 mm/min. The steel loading plate with a diameter of 20 cm and a thickness of 3 cm was used, and it was placed in the center of the stone column. The data-acquisition systems included the computer, data logger, and four sensors. Two linear variable differential transformer (LVDT) were placed on the loading plate to record the displacement data. They measured any probable rotation occurring on the loading plate. Figure 1 shows a schematic diagram of an experimental setup with or without a blanket. The load cell employed was class S with a capacity of 3000 kg for measuring total force on a loading plate and a miniature load cell with a capacity of 500 kg mounted on top of the stone column for measuring stone column bearing force. Figure (2a) illustrates the loading frame and server motor. Figure (2b) shows the loading plate and sensors for experimental tests.

All tests were carried out until the full penetration of 50 mm displacement was achieved. In total, 16 tests were performed, and it is noted that some repeated tests were performed to ensure that the results are repeatable and consistent. Table 1 summarizes the experimental test details.

2 Materials Properties

2.1 Clay and Stone Materials

Clay beds were prepared using a locally available soil. Table 2 represents its properties in experimental tests. To determine the moisture content corresponding to 15 kPa of the undrained shear strength of the clay, a series of unconfined compressive strength tests were carried out on a cylindrical specimen with a diameter of 38 mm and a height of 90 mm. These tests were carried out on different water-content percentages according to ASTM D2166. Figure 3 illustrates the undrained shear strength versus various water-content percentages in clay. It can be seen that the required water-content percentage is 26 to reach an undrained shear strength of 15 kPa. It must be noted that to ensure the water-content percentage required for achieving an undrained shear strength of 15 kPa, an unconsolidated undrained triaxial test was also performed on a cylindrical sample with a diameter of 100 mm in 26% water content, based on ASTM D2850. The triaxial test results are in a good agreement with unconfined compression test results.

Table 3 describes the properties of stone material, and Fig. 4 shows the particle-size distribution for stone columns and clay materials. Crushed stone materials ranging from 2 to 10 mm were used for the stone column materials. D_{10}, D_{50}, and D_{90} are 3.4, 6.4, and 9.1 mm, respectively. The dry unit weight of 16kN/m3 was chosen as the unit weight of the granular material for the stone column and blanket. The selected unit weight corresponds to relative density of 71%. The triaxial test with a diameter of 100 mm was conducted to determine the internal friction angle of the granular materials. The properties of the stone-column material are listed in Table 3.

The ratio of the average aggregate size ($D_{50} = 6.4$ mm) to the diameter of the stone columns (D = 60 mm) was approximately in a 1:10 scale representation of the prototype stone columns of 600 mm diameter and an average aggregate size of 64 mm. Also, the size of the crushed stone was chosen in accordance with the guidelines suggested by Nayak (1983) and Fattah et al. (2010), in which the particle size is approximately 1/6 to 1/7 of the diameter of the stone columns. A value of 1/6 for this ratio was considered adequate, based on the works of Fox
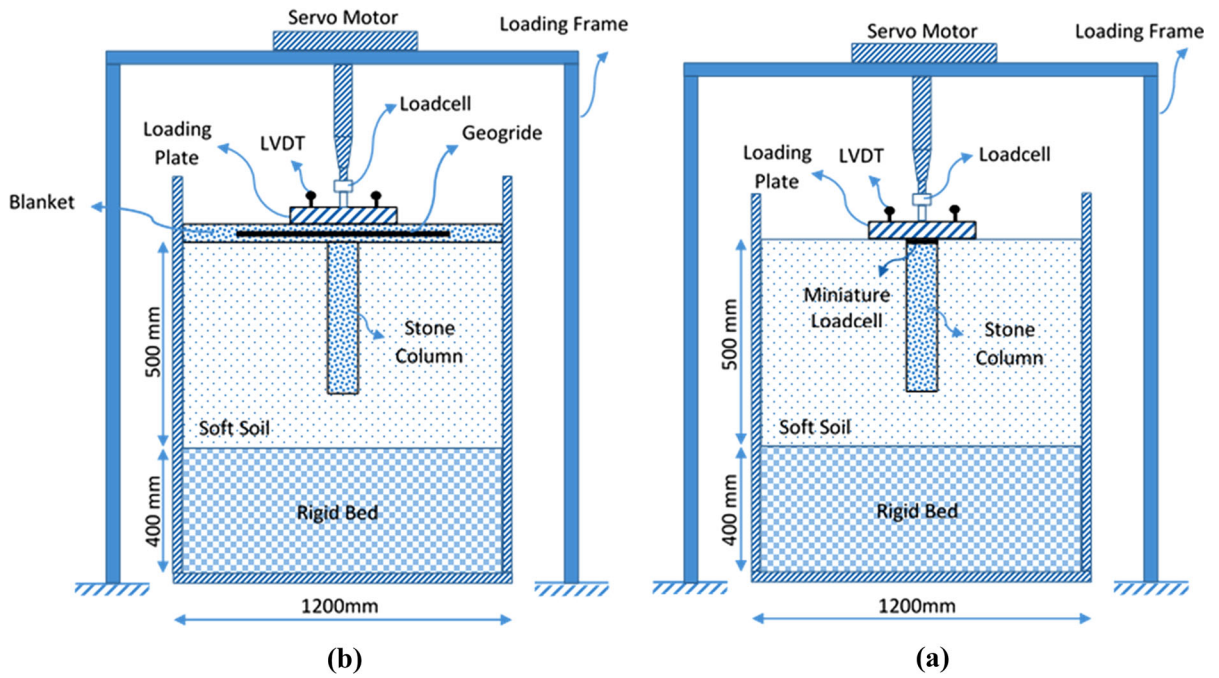
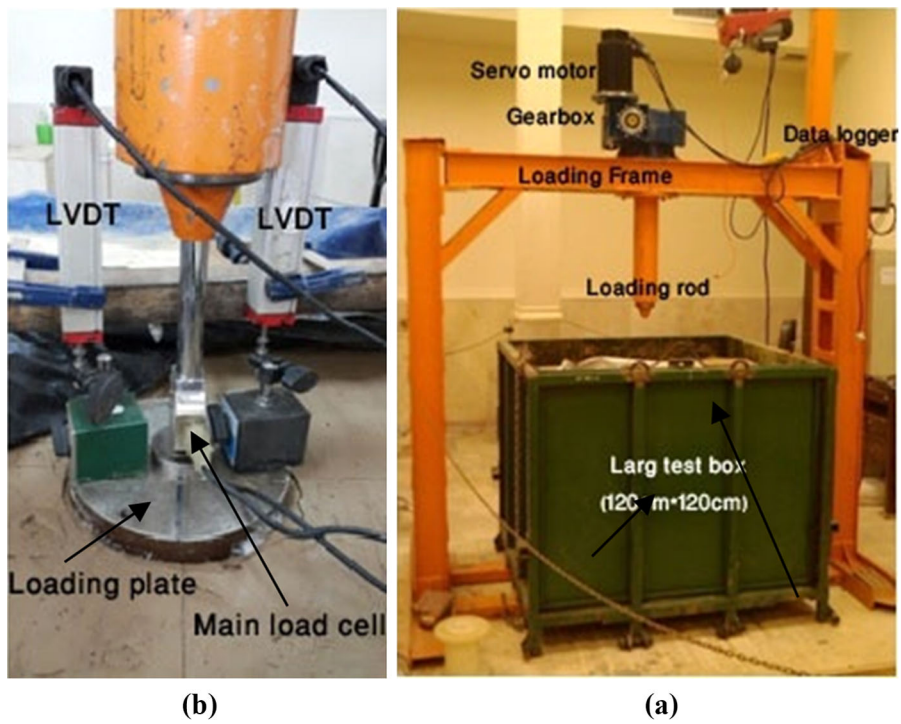**Fig. 1** Schematic diagram of test setup **a** without blanket and **b** with blanket

Fig. 2 Testing setup **a** loading frame and large test box **b** loading plate

Table 1 Summary of experimental program

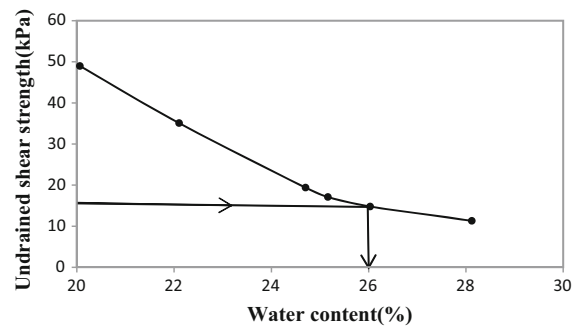| Test. no	Test name	Test description
1	Clay	
2	OSC	Ordinary stone column
3	ESC	Encased stone column
4	UB40	Unreinforced blanket with 40 mm thickness
5	UB75	Unreinforced blanket with 75 mm thickness
6	1RB40	One layered reinforced blanket with 40 mm thickness
7	1RB75	One layered reinforced blanket with 75 mm thickness
8	2RB75	Two layered reinforced blanket with 75 mm thickness
9	OSC-UB40	Ordinary stone column + Unreinforced blanket with 40 mm thickness
10	ESC-UB40	Encased stone column + Unreinforced blanket with 40 mm thickness
11	OSC-UB75	Ordinary stone column + Unreinforced blanket with 75 mm thickness
12	ESC-UB75	Encased stone column + Unreinforced blanket with 75 mm thickness
13	OSC-1RB40	Ordinary stone column + One layered reinforced blanket with 40 mm thickness
14	OSC-1RB75	Ordinary stone column + One layered reinforced blanket with 75 mm thickness
15	ESC-1RB75	Encased stone column + One layered reinforced blanket with 75 mm thickness
16	OSC-2RB75	Ordinary stone column + Two layered reinforced blanket with 75 mm thickness

Table 2 Properties of clay

Parameter	Value
Specific gravity	2.7
Liquid limit (%)	31
Plastic limit (%)	18
Plastic index	13
Optimum moisture content (%)	17
Maximum dry unit weight	16.5 kN/m3
Bulk unit weight at 26% water content	19.5 kN/m3
Undrained shear strength at 26% water content	15 kPa
USCS classification symbol	CL

Fig. 3 Variation of undrained shear strength of clay with water content

(2011), Stoeber (2012), and Mohapatra et al. (2016), in which a ratio of approximately 6 for the triaxial specimen diameter to maximum particle size was found to be satisfactory for granular material. In this research, the diameter of the stone column is 60 mm, so the maximum size of the stone column material is limited to 10 mm.

2.2 Reinforcement Properties

The type of reinforcement is determined with respect to the effect of the model scale. Based on the scale effect rules presented by Iai (1989) and discussed by Dash and Bora (2013a), Ghazavi and Nazariafshar

(2013), and Hong et al. (2016), the relationship between the prototype and model reinforcement stiffness can be calculated using Eq. (1).

$$J_p = J_m \cdot \lambda^2 \qquad (1)$$

Where J_p is prototype-reinforcement stiffness, J_m is model-reinforcement stiffness, and $1/\lambda$ is the model scale that in this research λ is 10.

In most projects, geotextile stiffness varies between 50 and 2000 kN/m, and geogrid stiffness is below 4000 kN/m (Huesker and Tencate, Hong et al. 2016). Because the scale parameter $\lambda = 1/10$ was used in this research, the reinforcement stiffness was selected and applied based on the scale effect. Table 4 describes the properties of reinforcements.

Table 3 Properties of stone column material

Parameter	Value
Specific gravity	2.6
Maximum dry unit weight	16.7 kN/m3
Minimum dry unit weight	14.5 kN/m3
Bulk unit weight for test at 71% relative density	16 kN/m3
Internal friction angle at 71% relative density	47°
Uniformity coefficient	2
Curvature coefficient	1.23
USCS classification symbol	GP
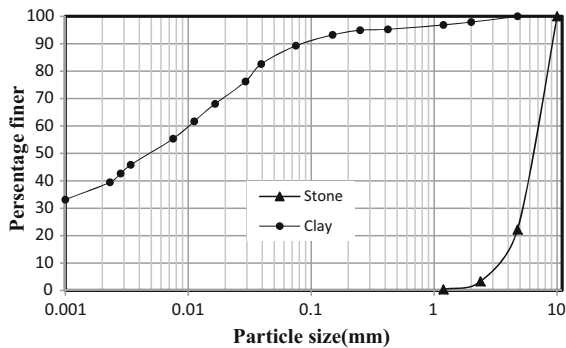
Fig. 4 Particle size distribution for stone column and clay materials Geotextile Encasement

3 Construction of Physical Models

3.1 Preparation of Clay Bed

Clay was sieved with a 1 cm aperture to separate any impurities and lumps. Two layers of thick nylon were used to prevent any water content reduction inside the preparation boxes. Primary clay water content was accurately measured to estimate the water required to reach a water content of 26%. The clay was placed in the preparation box in the form of 1 cm layers. The water required to reach water content of 26% was steadily spattered over each layer using a special sprinkler. Then, the sample was covered by nylon and left for one week to reach equal water content. To ensure a soil water content of 26%, a water-content test was performed on soil samples from various parts of soil boxes. To control the thickness of each layer, the main box wall was graded in 5 cm intervals so soft clay samples could be constructed in 5 cm layers using the unit-weight-control method. Before carrying out any tests, the main box walls were coated by a thin layer of grease to reduce any friction between the clay and the walls. To reach a unit weight of 19.5 kN/m^3, clay was weighed, and it was placed into the main box in the form of 5 cm layers. The layers were compacted using a special hammer (150 mm × 150 mm and w = 10 kg). Five steel bars with a diameter of 10 mm and a length of 20 mm were placed under the special hammer for kneading each clay layer. This helped to reduce leftover air voids in the test bed and to connect clay layers to one another. Each soil layer was compacted to reach 50 cm in height, and the final soft clay surface was leveled and trimmed to have a proper surface without any cavities. This construction method was replicated for all the experimental tests. Throughout the course of the experiments, the water content was measured to ensure the desired percentage of

Table 4 Properties of geogrid and geotextile

Parameter	Geotextile	Geogrid
Yarn material	Polypropylene	Polypropylene
Ultimate tensile strength (kN/m)	9	6.5
Strain at ultimate strength (%)	55	38.6
Stiffness at ultimate strain (J) (kN/m)	16.36	16.84
Thickness(mm)	1	2
Mass (g/m^2)	140	–
Mesh aperture(mm)	–	25

water. The results showed that the water-content percentage variations were below 1% in all tests. To further reassure the undrained strength of the soft clay sample after each test, an unconfined compression test was carried out on samples. In all the unconfined compression tests, the results approved the presence of the undrained shear strength of 15 kPa, and the water content was 26%.

3.2 Construction of Reinforced and Unreinforced Stone Columns

A floating stone column with a diameter of 60 mm and a length of 350 mm was used in this study. Stone columns were reinforced using geotextile. All stone columns were constructed with the replacement method in the center of the main large box. To construct the stone columns, a hollow steel open-ended pipe without any seam was used with a diameter of 60 mm and a thickness of 2 mm. In all tests, the internal and external areas of the steel pipe were coated by oil to reduce the surrounding soil manipulation and also to place the soil inside it easily. The hollow pipe was then vertically settled on the clay and pushed into it. During this procedure, the vertical state was carefully controlled by a special level. After reaching 350 mm in depth, the soil inside was discharged using a steel spiral auger. The diameter of the auger was smaller than the inner diameter of the pipe. In each step, soil with a maximum thickness of 50 mm was removed. After that, the pipe was pulled out slowly without any deviation from its vertical state. The stone column materials were then weighted and placed into the hole and compacted to reach the thickness of 0.5D (with D being the diameter of the stone column). In all tests, the unit weight of the stone column materials was $16 kN/m^3$. To achieve a uniform density, a steel circular tamper with a weight of 2 kg and a diameter of 20 mm was employed. Figure (5a) illustrates an unreinforced stone column, and Fig. (5b) shows a reinforced stone column, respectively.

To construct a reinforced stone column, nonwoven polypropylene geotextile was first cut into a rectangular form. It was constructed in cylindrical form with thermal glue made of polypropylene. The extent of geotextile overlap on the seam was 1.5 cm. It should be mentioned that tension tests confirmed the adequacy of this type of joint. It indicated that the presence of a seam coated by the thermal glue to make a geotextile encasement had no adverse effect on the geotextile strength (Fig. 6). After construction, the steel pipe was encased by geotextile reinforcement, and the reinforcement was pushed into the soft clay with the pipe. To prevent the displacement of the reinforcement, an appropriate joint was created at the bottom of the column. Granular materials were then placed and compacted as previously described.

3.3 Constructing Reinforced and Unreinforced Granular Blankets

Stone column materials were used to construct the granular blankets. The blanket thicknesses were 40 and 75 mm. Granular materials were weighed to reach a unit weight of $16 kN/m^3$ and the half thickness of the blankets. They were then placed over the soft clay and compacted using a cylindrical hammer (10 mm in diameter) made of polypropylene to reach the specified thickness. In the previous studies, an optimum length was shown for the reinforcements (Guido et al. 1986; Omar et al. 1993; Latha and Somwanshi 2009; Deb et al. 2011). They concluded that lengths over the optimum value do not have a positive effect to increase bearing capacity. This length is about 2–8 times the diameter or the width of the loading plate. Apparently, the optimum length of the reinforcements depends on such conditions as the number of reinforcing layers, the type of soil, and the soil density. For instance, Mosallanezhad et al. (2010) demonstrated that, as the number of the reinforcing layers increases, its optimum length will also increase. In the present research, geogrids in the form of squares with lengths of 3 times the diameter of the loading plate were used to reinforce the granular blanket. They were placed in the middle of the blanket layer and, in sample 2RB75, the vertical distance of 25 mm between geogrid layers was considered.
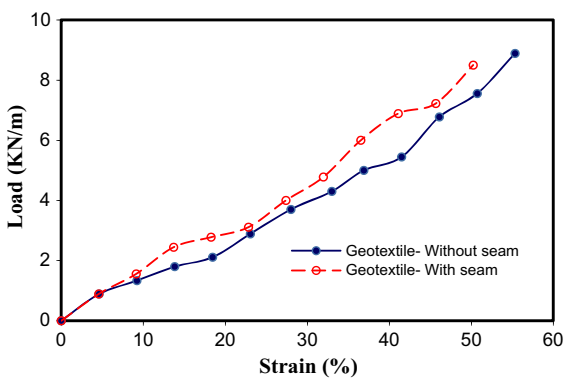
4 Results and Discussion

4.1 Load-Settlement Behavior

Figure 7 illustrates the load-settlement curves of the clay bed, the improved ground by the stone column, and the reinforced stone column. According to Fig. 7, stone columns increased bearing capacity of soft soil

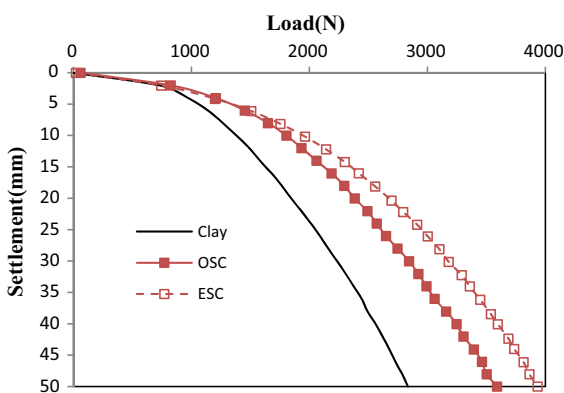**(a)**   **(b)**
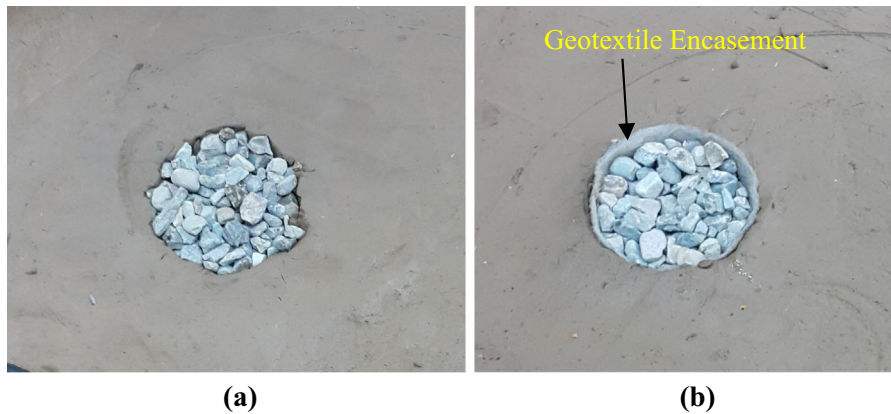
Fig. 5 Plan view of **a** unreinforced stone column **b** reinforced stone column


Fig. 6 Tensile load-strain behavior of geotextile samples with and without seam

up to 27% in 50 mm settlement and increased to 39% using reinforced stone columns. In fact, lateral pressure increased as geotextiles were used around the

stone column, and geotextiles prevented the stone-column materials from sinking into the soft soil; therefore, bearing capacity increases. Figure 8 illustrates the load-settlement curves of reinforced and unreinforced granular blankets. As indicated, the bearing capacity increased as the granular blanket thickness increased. The granular blankets with 40 and 75 mm thicknesses increased the bearing capacity respectively at 19 and 33% in the 50 mm settlement. A comparison of stone columns and unreinforced granular blankets showed that stone columns are more economical than unreinforced granular blankets. This is because the volume of materials used in 40 and 75 mm granular blankets is 58 and 109 times the volume of materials used in stone columns, respectively, in these tests. In addition, because of the high permeability of stone materials, stone columns speed up the consolidation rate in soft soils and are useful in

Fig. 7 Load-settlement variation of reinforced and unreinforced stone columns
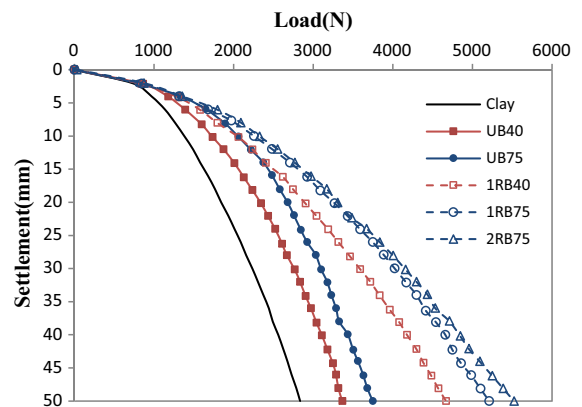
Fig. 8 Load-settlement variation of reinforced and unreinforced blankets

terms of drainage and in decreasing the potential of liquefaction.

According to Fig. 8, the bearing capacity increases to 65 and 85% if a layer of geogrid reinforcement is used in 40 mm (Test 1RB40) and 75 mm (Test 1RB75) granular blankets, respectively. This is because geogrids have relatively high axial tensile strengths, and soil grains are locked with geogrid ribs, which mobilize high frictional strength at the geogrid-soil interface. Additionally, the vertical stress is reduced in the zone below the reinforcement because of the combined action of mobilized tension in the reinforcement and membrane action in its curvature (Burd 1995; Lee et al. 1999; Basudhar et al. 2008; Deb et al. 2011). At a low granular-blanket thickness, a large extension has occurred in the geogrid reinforcement directly underneath the footing so that, as the thickness of the granular blanket increases, the ultimate capacity increases. When the granular blanket thickness increases, a major portion of the shear failure zone of the soil is developed above the reinforcement layer, the extension of the reinforcement decreases, and the effectiveness of the reinforcement also decreases (Lee et al. 1999; Deb et al. 2011). Using two reinforcement layers in granular blankets with 75 mm thickness (Test 2RB75) did not significantly increase the bearing capacity in comparison with one reinforcement layer. The optimum distance between geogrid layers is between 0.2 and 0.33 times the loading plate (Omar et al. 1993; Yetimoglu et al. 1994; Zidan 2012). In this research, the vertical distance between geogrid layers in Test 2RB75 is 0.12 times the loading plate that is below the optimum value. Because of interference between shear bands, the geogrid layer interfered with the surrounding soil, and bearing capacity did not significantly increase in comparison to one reinforcement layer. These results are also consistent with those obtained by Das and Khing (1994), Chakraborty and Kumar (2014), and Abu-Farsakh et al. (2013). According to Fig. 9, the simultaneous application of stone columns and granular blankets is more effective than the application of any of these methods alone. The combinations that used a reinforced blanket on top of stone columns proved to be most effective. This not only causes vertical and horizontal drainage, but also significantly increases ultimate bearing capacity. As a result, the granular blanket behaves as a subgrade supported beam and stands effectively against the loading plate,

leading to improved performance of the stone columns. Bearing capacity of ordinary stone columns using unreinforced, one-layer and two-layer reinforced 75 mm thickness blankets, as compared to unimproved clay beds, increases 57% (Test OSC-UB75), 105% (Test OSC-1RB75), and 117% (Test OSC-2RB75), respectively. The bearing capacity of ordinary stone columns using unreinforced and one-layer reinforced 40 mm thickness blankets, as compared to unimproved clay beds, increased 40% (Test OSC-UB40) and 84% (Test OSC-1RB40), respectively. As compared in Figs. 7 and 9, using a 40 cm unreinforced granular blanket on top of an ordinary stone column (Test OSC-UB40) is similar to a reinforced stone column (Test ESC), so we can use an unreinforced granular blanket with a thickness of 0.2 times that of a loading plate instead of a reinforced stone column. This is important if a reinforced stone column is not practicable.

4.2 Load Ratio Parameter

For better comparison of the test results, load ratio (LR) curves are presented in Figs. 10 and 11. Load ratio parameter is defined as:
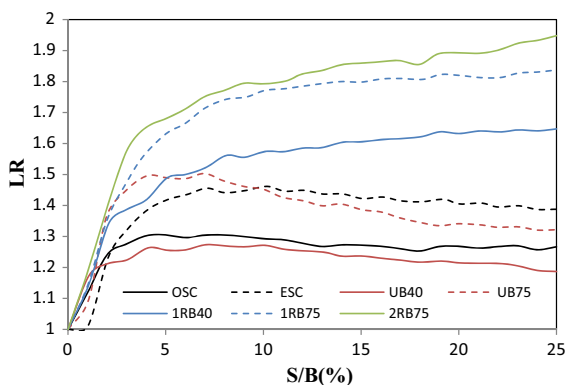
$$LR = \frac{\text{Ultimate load obtained from reinforced soil}}{\text{Ultimate load obtained from soft soil with no reinforcement}}$$

Figure 10 shows the curves of the LR of stone columns and granular blankets separately. Figure 11 shows the loading ratio curves of a combination of stone columns and granular blankets. In those
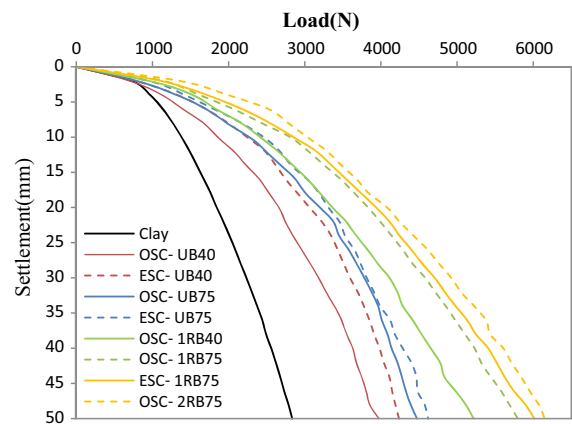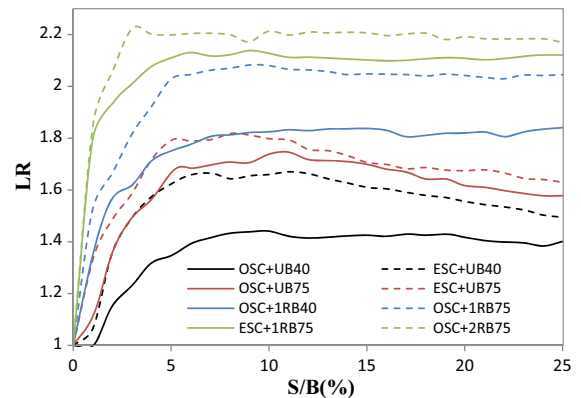

Fig. 9 Load-settlement variation of combination of granular blankets and stone columns

diagrams, (S/B) is penetration ratio and refers to the ratio of settlement (S) to the diameter of the loading plate (B). According to Fig. 10, the maximum LRs of ordinary stone columns (Test OSC) and encased stone columns (Test ESC) are, respectively, 1.30 and 1.46, which shows an effective application of geotextile encasement around the stone columns. In addition, the maximum LRs of 40 and 75-mm thickness unreinforced granular blankets (Test UB40 and Test UB75) were respectively 1.27 and 1.5, which shows that these blankets are similar to the Test OSC and Test ESC, respectively. Similar results are given in Figs. 7 and 8. It can be noted that stone columns speed up the consolidation rate in saturated soft soils and are useful in terms of drainage and in decreasing the potential of liquefaction, but these beneficial aspects are not provided with granular blankets. The maximum LRs in one layer of reinforced 40 mm (Test 1RB40) and 75 mm granular blankets (Test 1RB75) were, respectively, 1.64 and 1.83, which shows effective application of the geogrid in granular blankets. The LR of the two reinforced layers increased to 1.94 in 75 mm granular blankets (Test 2RB75) and did not significantly increase the bearing capacity in comparison with one reinforcement layer. The LR of the unreinforced granular blanket increased to a maximum value and then, at 8% penetration ratio, decreased. However, the LR of the reinforced granular blanket did not decrease at a high penetration rate. Generally, it is observed that the highest rate of increase in the LR charts occurred before reaching a 5% penetration ratio. After that, the value of the LR was generally constant.

Fig. 11 Variation of load ratio versus penetration ratio for combination of stone column and blanket

It was also noted that, by using reinforcement materials in stone columns or granular blankets, the rate of increase in the LR value rose from the increase in the stone column stiffness.

According to Fig. 11, the LR increases as a combination of stone columns and granular blankets are used. Figure 11 shows that reinforced stone columns under 40 mm granular blankets increased the maximum LR from 1.44 to 1.67 (Test OSC-UB40 compared to Test ESC-UB40). Reinforcement of stone columns under 75 mm granular blankets increased the maximum LR from 1.74 to 1.82 (Test OSC-UB75 compare to Test ESC-UB75). However, reinforcing the 40 mm granular blanket over the stone column increased the maximum LR from 1.44 to 1.84 (Test OSC-UB40 compared to Test OSC-1RB40). Reinforcement of the 75 mm granular blankets over the stone columns increased the maximum LR from 1.74 to 2.09 (Test OSC-UB75 compared to Test OSC-1RB75). As a result, using reinforced stone columns under thinner granular blankets significantly improved the efficiency of a combination of stone columns and granular blankets. However, it required less stone column reinforcement when thicker granular blanket were used. Reinforcing the granular blankets improved the efficiency of a combination of stone columns and granular blankets. It is noted that using a combination of stone columns and granular blankets increased the rate of the LR value by increasing the test stiffness and also using reinforcement materials in the stone columns, and the granular blankets further increased the stiffness of the test.


Fig. 10 Variation of load ratio versus penetration ratio for stone column and blanket

4.3 Stress Concentration Ratio

The external load is distributed between stone columns and soft soil in terms of the ratio of the column stiffness to that of the soft soil. Because stone columns are stiffer than the surrounding clay, the stresses on the columns are greater than on the surrounding soil. Fattah et al. (2010), Murugesan and Rajagopal (2010), and Ghazavi and Nazariafshar (2013) measured the stress imposed on the stone column and the surrounding soil to study the stress-concentration ratio in stone columns. The load on the stone columns is an important criterion on the effectiveness of stone columns and is used in their design. The stress concentration ratio is defined as:

$$n = \frac{\text{Stress in stone column}}{\text{Stress in soft clay surrounding stone column}}$$

In this study, a hole was located at the back and at the center of the loading plate to place a miniature load cell on the stone column and measure the load on the stone column, which was used to measure the stress-concentration ratio. The loading capacity of the stone column at each settlement can be measured using the miniature load cell. It is noteworthy that the load on the soil around the stone columns was measured by the difference between the main load and the load on the stone columns at each settlement.

According to Fig. 12, using geotextile encasement increases the stress concentration ratio (n) in stone columns. The maximum value of n was increased from 3.9 in ordinary stone columns to 4.9 in reinforced stone columns. In fact, bulging decreased as geotextile encasement was used, which is an important factor in increasing the bearing capacity of stone columns. Moreover, the stress concentration ratio reached to a maximum value at a 10% penetration ratio and consequently decreased. A value of n 16% decrease in ordinary stone column and 10% decrease in reinforced stone columns occurred. A decrease in the stress concentration ratio at a higher than 10% penetration ratio is due to the failure of the stone column materials because of bulging or the materials sinking into the surrounding soil. In addition, the stiffness of the reinforcement around the stone columns increased with increasing the penetration ratio. Therefore, a decrease of the stress concentration ratio in reinforced stone columns is less than in ordinary stone columns because there is less bulging
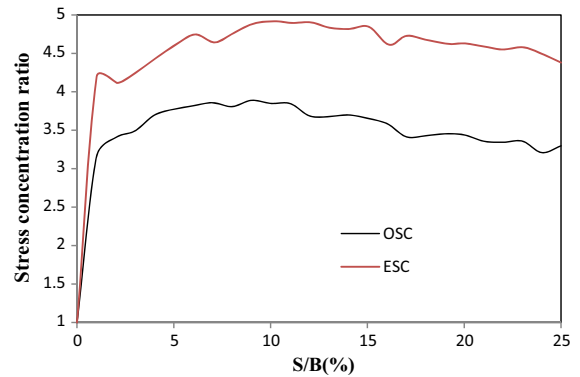
Fig. 12 Verification of stress concentration ratio versus penetration ratio for samples

and a lack of penetration of the stone column materials into the soil around the reinforced stone columns.

5 Conclusions

In this study, large-scale experimental tests were conducted on stone columns, granular blankets, and a combination of stone columns and granular blankets. Two different thicknesses (40 mm and 75 mm) of granular blankets were tested. Stone columns were reinforced with geotextiles, and granular blankets were reinforced with geogrid. According to the experimental tests, it can be concluded that:

1. In all cases, using granular blankets, stone columns, and a combination of both increased the ultimate bearing capacity. Simultaneous application of stone columns and granular blankets not only caused vertical and horizontal drainage, but also significantly increased the ultimate bearing capacity. Using geogrid in the reinforcement of granular blankets and using geotextiles in the reinforcement of stone columns improved the efficiency of stone columns and granular blankets.

2. The application of two layers of reinforcement in granular blankets with 75 mm thickness had no significant effect on the bearing capacity in comparison with the application of one layer of reinforcement. Because vertical distance between geogrid layers in Test 2RB75 was below the optimum value, and because of interference between shear bands, the geogrid layer interfered

with the surrounding soil, and the bearing capacity did not significantly increase.

3. Using stone columns is more economical than using unreinforced granular blankets. This is because the volume of materials used in 40 mm and 75 mm granular blankets is 58 and 109 times the volume of materials used in stone columns. In addition, because of high permeability of stone materials, stone columns speed up the consolidation rate in soft soils and are useful in terms of drainage and in decreasing the potential of liquefaction.

4. As a result, using reinforced stone columns under thinner granular blankets significantly improved the efficiency of a combination of stone columns and granular blankets. However, it was less required to reinforce stone columns if thicker granular blankets were used on the stone columns.

5. We can use an unreinforced granular blanket with a thickness of 0.2 times that of the loading plate instead of a reinforced stone column. This is important in the case that a reinforced stone column is not practicable.

6. The LRs of unreinforced granular blankets reach maximum values of an 8% penetration ratio, then consequently decrease. However, the LR would not decrease if a granular blanket was reinforced.

7. The maximum LR was observed in a combination of stone columns and reinforced granular blankets.

8. It has been observed that the highest rate of LR increase in charts occurs before reaching a 5% penetration ratio and, after that, the value of LR is approximately constant. Also, it is noted that, by using reinforcement material in stone columns or granular blankets, the rate of increase in LR value increases due to an increase in the stone column stiffness.

9. The application of geotextile encasement increases the stress-concentration ratio and bearing capacity in stone columns. Clearly, application of geotextile encasement decreases bulging, which effectively increases bearing capacity in stone columns.

References

Aboshi H, Ichimoto E, Harada K, Emoki M (1979) The composer e a method to improve the characteristics of soft clays by inclusion of large diameter sand columns. In: Proceedings of international conference on soil reinforcement, ENPC, 1, Paris, pp 211–216

Abu-Farsakh M, Chen Q, Sharma R (2013) An experimental evaluation of the behavior of footings on geosynthetic-reinforced sand. Soils Found J 53:335–348

Akinmusuru JO, Akinbolade JA (1981) Stability of loaded footing on reinforced soil. J Geotech Eng 107(GT6):819–827

Ali K, Shahu JT, Sharma KG (2014) Model tests on single and groups of stone columns with different geosynthetic reinforcement arrangement. Geosynth Int 21(2):103–118

Almeida MSS, Hosseinpour I, Riccio M (2013) Performance of a geosyntheticencased column (GEC) in soft ground: numerical and analytical studies. Geosynth Int 20(4):252–260

Andreou P, Papadopoulos V (2014) Factors affecting the settlement estimation of stone column reinforced soils. Geotech Geol Eng 32:1175–1185

Babu MD, Nayak S, Shivashankar R (2013) A critical review of construction, analysis and behaviour of stone columns. Geotech Geol Eng 31:1–22

Baker WE, Westine PS, Dodge FT (1991) Similarity methods in engineering dynamics: theory and practice of scale modeling, Revised edn. Elsevier Science Publishers BV, The Netherlands

Barksdale RD, Bachus RC (1983) Design and construction of stone column. Report No.FHWA/RD-83/026. National Technical Information Service, Springfield, Virginia

Basudhar PK, Dixit PM, Gharpure A, Deb K (2008) Finite element analysis of geotextile-reinforced sand-bed subjected to strip loading. Geotext Geomembr 26:91–99

Burd HJ (1995) Analysis of membrane action in reinforced unpaved roads. Can Geotech J 32:946–956

Chakraborty M, Kumar J (2014) Bearing capacity of circular foundations reinforced with geogrid sheets. Soils Found 54:820–832

Chummar AV (1972) Bearing capacity theory from experimental results. J Soil Mech Found Div ASCE 98(12):1311–1324

Das BM, Khing KH (1994) Foundation on layered soil with geogrid reinforcement effect of avoid. Geotext Geomembr 13(8):545–553

Dash SK, Bora MC (2013a) Improved performance of soft clay foundations using stone columns and geocell-sand mattress. Geotext Geomembr J 41:26–35

Dash SK, Bora MC (2013b) Influence of geosynthetic encasement on the performance of stone columns floating in soft clay. Can Geotech J 50(7):754–765

Datye KR, Nagaraju SS (1975) Installation and testing of rammed stone columns. In: Proceedings of IGS Specialty Session, 5th Asian regional conference on soil mechanic and foundation engineering, Bangalore, India, pp 101–104

Deb K, Basudhar P, Chandra S (2010) Axi-symmetric analysis of geosynthetic-reinforced granular fill-soft soil system

with group of stone columns. Geotech Geol Eng 28:177–186

Deb K, Samadhiya NK, Namdeo JB (2011) Laboratory model studies on unreinforced and geogrid-reinforced sand bed over stone column-improved soft clay. Geotext Geomembr 29:190–196

Elsawy MBD (2013) Behavior of soft ground improved by conventional and geogridencased stone columns, based on FEM study. Geosynth Int 20(4):276–285

Fakher A, Jones CJ (1996) Discussion: bearing capacity of rectangular footings on geogrid-reinforced sand. J Geotech Eng 122:326–327

Fattah MY, Shlash KT, Al-Waily MJM (2010) Stress concentration ratio of model stone columns in soft clays. Geotechn Test J. 34(1), Paper ID GTJ103060, ASTM, Nov 29 14:27:16 EST

Fox ZP (2011) Critical state, dilatancy and particle breakage of mine waste rock. Master's Thesis. Colorado State University, Fort Collins, USA

Ghazavi M, Nazariafshar J (2013) Bearing capacity of geosynthetic encased stonecolumns. Geotext Geomembr 38:26–36

Gniel J, Bouazza A (2008) Improvement of soft soils using geogrid encased stone columns. Geotext Geomembr 27(3):167–175

Greenwood DA (1970) Mechanical improvement of soils below ground surface. In: Proceedings of ground improvement conference. Institute of Civil Engineering, pp 9–29

Guido VA, Biesiadecki GL, Sullivan MJ (1985) Bearing Capacity of a Geotextile Reinforced Foundation. In: Proceedings of 11th international conference on soil mechanic and foundation engineering, San Francisco, California, pp 1777–1780

Guido VA, Chang DK, Sweeny MA (1986) Comparison of geogrid and geotextile reinforced slabs. Can Geotech J 20:435–440

Hong YS, Wu CS, Yu YS (2016) Model tests on geotextile-encased granular columns under 1-g and undrained conditions. Geotext Geomembr J 44:13–27

Hughes JMO, Withers NJ (1974) Reinforcing of soft cohesivesoils with stone columns. Ground Eng 7(3):42–49

Iai S (1989) Similitude for shaking table tests on soil-structure fluid models in 1g gravitational field. Soils Found 29(1):105–118

Latha GM, Somwanshi A (2009) Bearing capacity of square footings on geosynthetics reinforced sand. Geotext Geomembr 27(4):281–294

Lee KM, Manjunath VR, Dewaikar DM (1999) Numerical and model studies of strip footing supported by a reinforced granular fill-soft soil system. Can Geotech J 36:793–806

Madhav MR, Vitkar RP (1978) Strip footing on weak clay stabilized with a granular trench or pile. Can Geotech J 15(4):605–609

Madhav MR, Iyengar NGR, Vitkar RP, Nandia A (1979) Increased bearing capacity and reduced settlements due to inclusions in soil. In: Proceedings of international conference on soil reinforcement: reinforced and other techniques, pp 239–333

Mayerhof GG, Sastry VVRN (1978) Bearing capacity of piles in layered soils: part 2. Can Geotech J 15(2):183–189

McCabe B, Kamrat-Pietraszewska D, Egan D (2013) Ground heave induced by installing stone columns in clay soils. ICE Geotech Eng 166(6):589–593

Mckelvey D, Sivakumar V, Bell A, Graham J (2004) Modeling vibrated stone columns in soft clay. J Geotech Eng 157(3):137–149

Miranda M, Costa AD (2016) Laboratory analysis of encased stone columns. Geotext Geomembr 44:269–277

Mohapatra SR, Rajagopal K, Sharma J (2016) Direct shear tests on geosynthetic-encased granular columns. Geotext Geomembr J 44:396–405

Mosallanezhad M, Hataf N, Ghahramani A (2010) Three dimensional bearing capacity analysis of granular soil, reinforced with innovative grid-anchor system. Iran J Sci and Technol Trans B Eng 34(B4):419–431

Muir Wood D, Hu W, Nash DFT (2000) Group effects in stone column foundations—model tests. Geotechnique 50(6):689–698

Murugesan S, Rajagopal K (2006) Geosynthetic-encased stone columns: numerical evaluation. Geotext Geomembr J 24(6):349–358

Murugesan S, Rajagopal K (2010) Studies on the behavior of single and group of geosynthetic encased stone columns. J Geotech Geo Environ Eng ASCE 136(1):129–139

Nayak NV (1983) Recent advances in ground improvements by stone column. In: Proceedings of Indian Geotechnical Conference, IGC-83, Madras, India, Vol 1, pp 5–19

Nazariafshar J, Ghazavi M (2014) Experimental studies on bearing capacity of geosynthetic reinforced stone column. Arab J Eng 39:1559–1571

Omar MT, Das BM, Puri VK, Yen SC (1993) Ultimate bearing capacity of shallow foundations on sand with geogrid reinforcement. Can Geotech J 20(3):435–440

Patra CR, Das BM, Atalar C (2005) Bearing capacity of embedded strip foundation on geogrid-reinforced sand. Geotext Geomembr 23(5):454–462

Raithel M, Kempfert H-G, Kirchner A (2002) Geotextile-encased columns (GEC) for foundation of a dike on very soft soils. In: Proceedings of the seventh international conference on geosynthetics, Nice, France, pp 1025–1028

Rao S, Prasad YVS, Hanumanta Rao V, (1992) Useof stone columns in soft marine clays. In: Proceedings of the 45th Canadian geotechnical conference, Toronto, Ont, October, pp 9/1–9/7

Selig ET, McKee KE (1961) Static and dynamic behaviour of small footings. J Soil Mech Found Div ASCE 87(6):29–47

Sivakumar V, Jeludine DKNM, Bell A, Glyn DT, Mackinnon P (2011) The pressure distribution along stone columns in soft clay under consolidation and foundation loading. Geotechnique 61(7):613–620

Stoeber JN (2012) Effects of maximum particle size and sample scaling on the mechanical behavior of mine waste rock; A critical state approach. Master's Thesis. Colorado State University, Fort Collins, USA

Stuedlein AW, Holtz RD (2013) Displacement of spread footings on aggregate pier reinforced clay. J Geotech Geoenviron Eng 140:36–45

Van Impe WF (1989) Soil improvement techniques and their evolution. Balkema, Rotterdam

Vesic AS (1972) Expansion of cavities in infinite soil mass. J Soil Mech Found Eng Div ASCE 98(SM3):265–290

Wong HY (1975) Vibroflotation-its effect on weak cohesive soils. Civil Eng (London) 82:44–76

Yetimoglu T, Wu JTH, Saglamer A (1994) Bearing capacity of rectangular footing on geogrid—reinforced sand. J Geotech Eng 120(12):2083–2099

Yoo C (2010) Performance of geosynthetic-encased stone columns in embankment construction: a numerical investigation. J Geotech Geoenviron Eng 136(8):129–139

Yoo C, Lee DY (2012) Performance of geogrid-encased stone columns in soft ground: full-scale load tests. Geosynth Int 19(6):480–490

Zhang Y, Chan D, Wang Y (2012) Consolidation of composite foundation improved by geosynthetic-encased stone columns. Geotext Geomembr 32(3):10–17

Zidan AF (2012) Numerical study of behavior of circular footing on geogrid- reinforced sand under static and dynamic loading. Geotech Geol Eng 30(2):499–510